Article

Molecular Cell

A Surveillance Function of the HSPB8-BAG3-HSP70 Chaperone Complex Ensures Stress Granule Integrity and Dynamism

Graphical Abstract

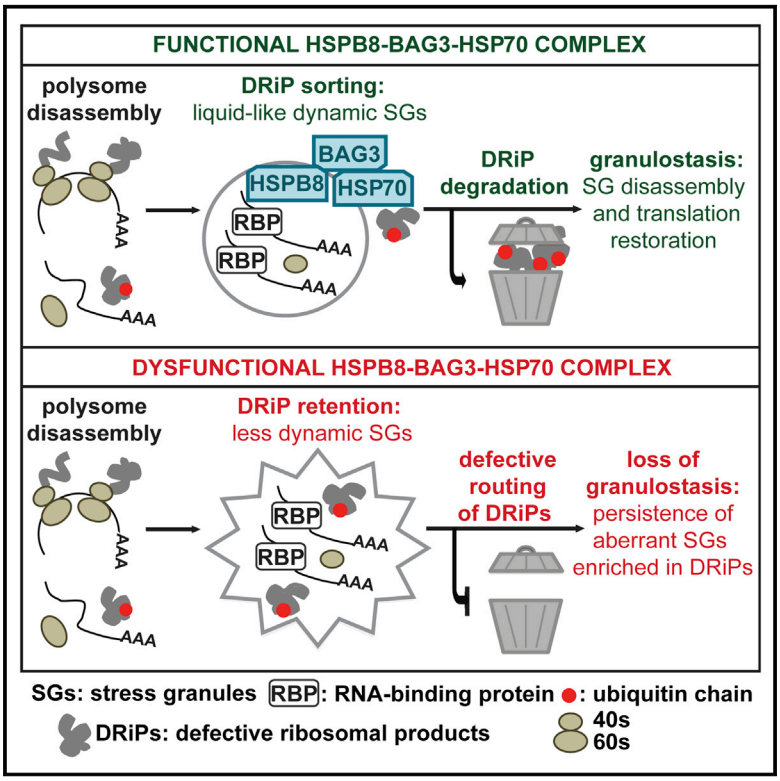

Highlights

- A fraction of stress granules accumulates DRiPs
- Accumulation of DRiPs alters the biochemistry, dynamics, and disassembly of SGs
- HSPB8-BAG3-HSP70 prevents DRiP accumulation in SGs
- Chaperone-mediated quality control maintains SG functionality

Authors

Massimo Ganassi, Daniel Mateju, Ilaria Bigi, ..., Angelo Poletti, Simon Alberti, Serena Carra

Correspondence

alberti@mpi-cbg.de (S.A.), serena.carra@unimore.it (S.C.)

In Brief

How pathological aggregates arise from physiological ribonucleoprotein granules is unknown. Ganassi et al. show that accumulation of defective ribosomal products in stress granules promotes their transition into an aberrant state and delays their disassembly, a process that is regulated by the coordinated action of the HSPB8-BAG3-HSP70 chaperone complex.

Ganassi et al., 2016, Molecular Cell *63*, 796–810
September 1, 2016
http://dx.doi.org/10.1016/j.molcel.2016.07.021

CellPress

Molecular Cell
Article

A Surveillance Function of the HSPB8-BAG3-HSP70 Chaperone Complex Ensures Stress Granule Integrity and Dynamism

Massimo Ganassi,[1,5] Daniel Mateju,[2,5] Ilaria Bigi,[1,5] Laura Mediani,[1] Ina Poser,[2] Hyun O. Lee,[2] Samuel J. Seguin,[1] Federica F. Morelli,[1] Jonathan Vinet,[1] Giuseppina Leo,[1] Orietta Pansarasa,[3] Cristina Cereda,[3] Angelo Poletti,[4] Simon Alberti,[2,*] and Serena Carra[1,6,*]

[1]Department of Biomedical, Metabolic and Neural Sciences, University of Modena and Reggio Emilia, Modena 41125, Italy
[2]Max Planck Institute of Molecular Cell Biology and Genetics, Dresden 01307, Germany
[3]Laboratory of Experimental Neurobiology, "C. Mondino" National Institute of Neurology Foundation, IRCCS, Via Mondino 2, 27100 Pavia, Italy
[4]Department of Pharmacological and Biomolecular Sciences, Centre of Excellence on Neurodegenerative Diseases University of Milan, Milan 20133, Italy
[5]Co-first author
[6]Lead Contact
*Correspondence: alberti@mpi-cbg.de (S.A.), serena.carra@unimore.it (S.C.)
http://dx.doi.org/10.1016/j.molcel.2016.07.021

SUMMARY

Stress granules (SGs) are ribonucleoprotein complexes induced by stress. They sequester mRNAs and disassemble when the stress subsides, allowing translation restoration. In amyotrophic lateral sclerosis (ALS), aberrant SGs cannot disassemble and therefore accumulate and are degraded by autophagy. However, the molecular events causing aberrant SG formation and the molecular players regulating this transition are largely unknown. We report that defective ribosomal products (DRiPs) accumulate in SGs and promote a transition into an aberrant state that renders SGs resistant to RNase. We show that only a minor fraction of aberrant SGs is targeted by autophagy, whereas the majority disassembles in a process that requires assistance by the HSPB8-BAG3-HSP70 chaperone complex. We further demonstrate that HSPB8-BAG3-HSP70 ensures the functionality of SGs and restores proteostasis by targeting DRiPs for degradation. We propose a system of chaperone-mediated SG surveillance, or granulostasis, which regulates SG composition and dynamics and thus may play an important role in ALS.

INTRODUCTION

Stress granules (SGs) are membrane-less ribonucleoprotein assemblies that form upon proteotoxic stress, when translation is inhibited (Kedersha and Anderson, 2002). SGs are enriched for RNA-binding proteins (RBPs), such as TIA-1, hnRNPA1, and FUS. These proteins contain RNA-binding domains and intrinsically disordered domains of low sequence complexity, which promote assembly into SGs (Gilks et al., 2004). Recombinant hnRNPA1 and FUS undergo liquid-liquid phase separation in vitro and form dynamic structures that resemble RNP granules in living cells. However, these liquid-like structures are unstable and mature with time into more solid hydrogels or fibers (Molliex et al., 2015; Murakami et al., 2015; Patel et al., 2015). These structures are reminiscent of pathological inclusions observed in amyotrophic lateral sclerosis (ALS) and frontotemporal dementia (FTD) (Robberecht and Philips, 2013).

There is increasing evidence that the formation of aberrant RNP granules plays a central role in ALS and FTD. In patients afflicted with these diseases, genetic mutations in TDP-43, FUS and hnRNPA1 were identified (Kim et al., 2013; Robberecht and Philips, 2013). These disease-linked mutations accelerate FUS and hnRNPA1 conversion from a liquid-like to an aggregated state (Molliex et al., 2015; Murakami et al., 2015; Patel et al., 2015). Altered SG dynamics may be a key pathogenic event, highlighting the necessity to define the mechanisms governing SG dynamics in cells.

Pathological inclusions in ALS patients contain SG proteins like eIF3 and TIA-1 (Liu-Yesucevitz et al., 2010), suggesting that pathological inclusions may arise from SGs and that SGs may undergo a slow maturation process that culminates in the formation of pathological aggregates. This raises three important questions: What are the mechanisms regulating SG assembly? What are the molecular events causing aberrant SG formation? And what prevents the conversion into pathological aggregates in young cells?

A potential explanation comes from the observation that SGs form when cells accumulate misfolded proteins, which may interact with SGs and change their dynamics (Kedersha and Anderson, 2002). Defective ribosomal products (DRiPs) are prematurely terminated polypeptides originating from the translation of bona fide mRNAs. DRiPs are the predominant source of misfolded proteins in living cells and are released by disassembling polysomes prior to SG formation (Meriin et al., 2012; Schubert et al., 2000; Yewdell, 2002). We previously showed that depletion of the chaperone VCP (valosin-containing protein) and its

co-factors UFD1L (ubiquitin fusion degradation protein 1-like) and PLAA (phospholipase A2-activating protein), which target DRiPs for degradation (Verma et al., 2013), results in the accumulation of DRiPs in the proximity of SGs and affects their dynamics (Seguin et al., 2014). Thus, defective sorting and degradation of DRiPs could promote the conversion of physiological SGs into pathological aggregates.

In agreement with a central role of misfolded proteins, an increasing number of patient mutations are identified in the protein quality control system (PQC), including chaperones, components of the ubiquitin/proteasome or autophagolysosomal system (Robberecht and Philips, 2013). Thus, PQC factors may survey SG composition to prevent their conversion into an aberrant state. Indeed, in yeast and fruit flies, chaperones of the Hsp70, Hsp110, or Hsp100 families promote the disaggregation of mixed aggregates that consist of misfolded proteins and SG components (Cherkasov et al., 2013; Kroschwald et al., 2015). However, the role of chaperones in mammalian cells is less clear. A previous report showed that genetic depletion of HSPA1A/HSP70 delays SG dissolution in mammalian cells (Mazroui et al., 2007), but the molecular basis of this observation remained unclear. We previously showed that HSP70, in concert with the nucleotide-exchange factor BAG3 and the small heat shock protein HSPB8, assists the degradation of ubiquitinated and misfolded proteins (Crippa et al., 2010; Minoia et al., 2014). Thus, we hypothesized that the HSPB8-BAG3-HSP70 chaperone complex could play a key role in SG quality control.

Here, we demonstrate that, when the HSPB8-BAG3-HSP70 chaperone complex is impaired, DRiPs accumulate in mammalian SGs and that DRiP accumulation gradually changes composition, dynamics, and disassembly kinetics of SGs. We further show that the majority of SGs disassemble with the assistance of the HSPB8-BAG3-HSP70 complex. Based on these findings, we propose a system of chaperone-mediated quality control, which regulates the accumulation of misfolded proteins inside SGs, thereby maintaining their dynamic behavior and ensuring proper translation restoration after stress.

RESULTS

SGs Assemble upon Various Stresses

Exposure of mammalian cells to environmental stress, such as oxidative stress (arsenite), heat shock, or proteasome inhibition, elicits the assembly of RBPs and mRNAs into SGs (Kedersha and Anderson, 2002). To test if different proteotoxic stress conditions yield SGs of similar microscopic and molecular behavior, we treated HeLa cells with arsenite or the proteasome inhibitor MG132. We visualized SGs by immunofluorescence with an antibody against TIA-1, a ubiquitous marker for SGs. Arsenite and MG132 induced SGs shortly after treatment (Figures S1A and S1B). These structures were bona fide SGs, because SG formation was blocked by co-treatment with cycloheximide, a translation elongation inhibitor (Figures S1A and S1B). Arsenite- and MG132-induced SGs disappeared 2 to 3 hr after drug removal (Figures S1A and S1B). In line with previous reports (Mazroui et al., 2007), SGs also disappeared during continuous treatment with MG132 for 6 to 8 hr (Figure S1C), suggesting that cells adapt to long-term MG132 treatment. Thus, SGs are reversible structures and dissolve shortly after release from stress or upon adaptation.

HSPA1A, but Not HSPA6, Assists SG Disassembly

Continuous proteasome inhibition also induces the chaperone HSP70/HSPA1A (Mazroui et al., 2007), which may explain the observed adaptation and dissolution of SGs. Accordingly, depletion of HSP70 increased the percentage of cells with persisting SGs upon prolonged MG132 treatment and delayed translation restoration. This suggests that HSP70 plays an important role in restoring protein homeostasis and that interference with HSP70 may generate a population of persisting SGs, which cannot easily dissolve.

To investigate if HSP70 function is required for SG dissolution, we manipulated HSP70 activity or expression. First, we depleted HSPA1A using a specific small interfering RNA (siRNA) (Figure S1D). Some HSPA1A was still detectable after 6 hr of MG132 treatment, suggesting that cells respond to proteasome inhibition with a strong HSPA1A upregulation, which partially overcomes the inhibitory action of the siRNA. However, even under these conditions, HSPA1A depletion significantly delayed SG disassembly (Figure 1A). We next blocked HSP70 activity with VER-155008 (VER), an ATP analog that binds to HSP70 nucleotide-binding domain and inhibits its ATPase activity. We observed that VER does not induce SGs or affect their assembly (Figure S1E and data not shown). This agrees with our finding that HSP70-depleted cells form SGs normally (Figure 1A) and suggests that HSP70 is not required for SG assembly per se. To assess the impact of HSP70 inhibition on SG disassembly, we induced SGs with MG132, and we allowed the cells to recover in absence or presence of VER. Cells recovering in control medium disassembled most SGs within 2 hr, yet a small number of persisting SGs was detectable (Figure 1B). However, in the presence of VER, the fraction of cells with persistent SGs was significantly increased (Figure 1B), demonstrating that chemical inhibition of HSP70 delays SG disassembly.

Along with HSPA1A, HSPA6/HSP70B′, another inducible member of the Hsp70 family, is strongly upregulated during proteotoxic stress (Noonan et al., 2007). We then asked if HSPA6/HSP70B′ also assists in SG disassembly. Depletion of HSPA6 did not affect SG assembly and disassembly in the presence of MG132 (Figure S1F) and translation restoration in HSPA6-depleted cells was similar to control cells (Figure S1G). These data support a specific role for HSP70/HSPA1A during SG disassembly.

Most SGs Dissolve in an Autophagy-Independent Manner

We noticed heterogeneity of SGs with respect to their ability to disassemble. One fraction of SGs disassembles over few hours, whereas some SGs persist for longer. Persisting SGs are particularly observed in HSPA1A-depleted cells and upon HSP70 inhibition with VER. This may result from defective SG disassembly or deficient targeting of SGs for degradation, or both. Because SGs can be degraded by autophagy (Buchan et al., 2013), we asked whether persisting SGs require autophagy for clearance. We inhibited autophagy using ammonium chloride (NH_4Cl), which blocks the activity of all lysosomal enzymes; in addition,

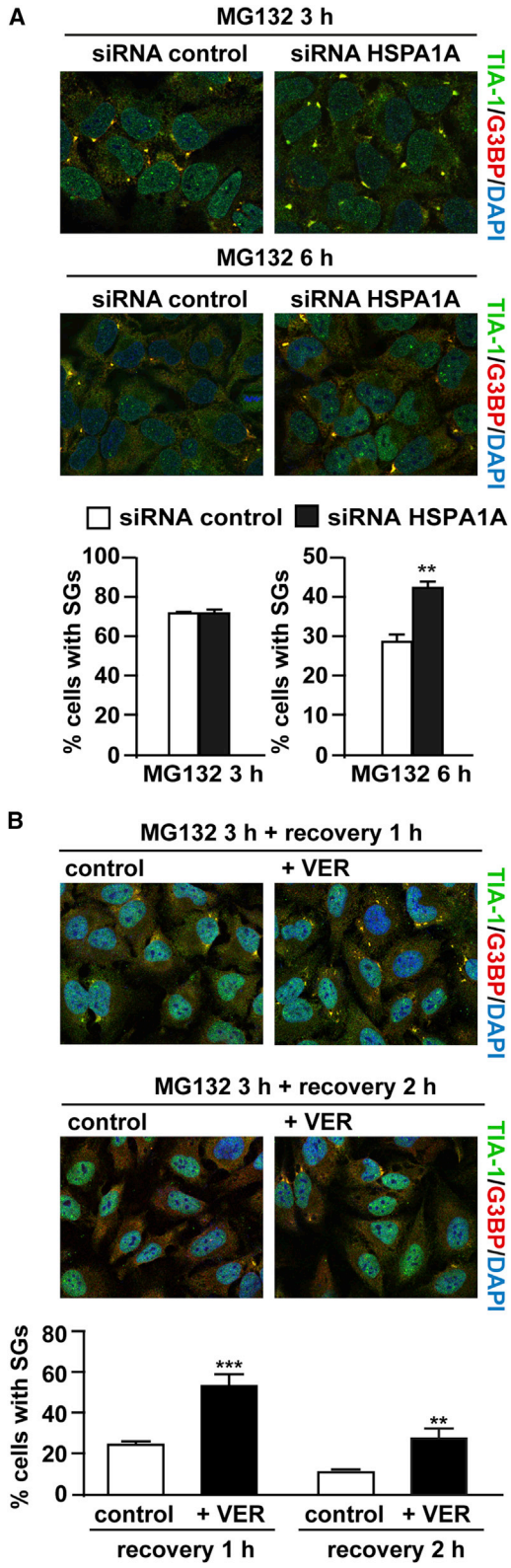

Figure 1. Inhibition of HSP70 Delays SG Disassembly

(A) HeLa cells were lipofected with HSPA1A or nontargeting siRNA control for 72 hr. Then, cells were treated with MG132, 20 μM, for 3 or 6 hr. Cells were fixed and stained for anti-TIA-1 and G3BP and the percentage of cells with SGs was counted. n = 4/condition, ± SEM; **p < 0.01.

(B) Immunofluorescence of cells treated with MG132 followed by recovery for 1 or 2 hr in absence or presence of VER 40 μM. Quantitation of % of cells with SGs. n = 4/condition, ± SEM; **p < 0.01.

See also Figure S1.

we used the lysosome inhibitors E64d and Leupeptin (Klionsky et al., 2016). Treatment of HeLa cells with NH_4Cl or E64d and Leupeptin per se did not induce SGs (Figure S2A). Surprisingly, addition of NH_4Cl or E64d and Leupeptin did not inhibit SG disappearance in cells treated with MG132 for prolonged times, despite the fact that the autophagy marker LC3-II was induced (Figure 2A; Figure S2A). When NH_4Cl was added after MG132 removal in the recovery time, we observed a small but significant delay in SG disappearance in roughly 10% of the cells (Figure 2B; Figure S2B), suggesting that only few SGs are degraded by autophagy. In agreement with this, the protein levels of the SG markers TIA-1 and TDP-43 were unchanged (Figures 2A and 2B). SG disassembly in the presence of lysosome inhibition was confirmed by live imaging of HeLa cells expressing G3BP2-GFP (Patel et al., 2015; Poser et al., 2008) (Figure 2C; Movie S1). These results demonstrate that only a minor fraction of SGs is degraded by autophagy, whereas the majority of SGs is disassembled in a chaperone-mediated/autophagy-independent fashion.

Inhibition of HSP70 Causes Accumulation of DRiPs in SGs that Persist

DRiPs are the main source of misfolded proteins in cells and are released by disassembling polysomes prior to SG formation (Meriin et al., 2012; Schubert et al., 2000; Yewdell, 2002). DRiPs are aggregation-prone, ubiquitinated, and degraded by proteasome or autophagy with assistance by chaperones, such as VCP (Verma et al., 2013) and HSP70 (Wegrzyn and Deuerling, 2005). We previously showed that DRiPs accumulate within or adjacent to SGs when autophagy is impaired or when VCP is depleted. Accumulation of DRiPs adjacent to or inside SGs correlated with delayed SG disassembly (Seguin et al., 2014). Thus, accumulation of misfolded proteins in SGs may change their dynamics and render them persistent.

We hypothesized that chaperones like HSP70 prevent DRiP accumulation inside SGs and, by doing so, facilitate the disassembly of DRiP-containing SGs. To investigate this, we first verified that HSP70 promotes DRiP clearance. We incubated HeLa cells with puromycin to label DRiPs. In line with the literature (Schubert et al., 2000), bortezomib impaired DRiP degradation and increased the fraction of DRiPs 2-fold compared with control cells (Figure S2C). Inhibition of HSP70 with VER also significantly increased the amount of DRiPs (Figure S2C), suggesting HSP70 involvement in DRiP processing. We then investigated if HSP70 inhibition leads to the accumulation of DRiPs inside SGs, using a high content imaging-based assay (see Experimental Procedures). Cells treated with VER contained MG132-induced SGs with a significantly greater amount of DRiPs (Figures 3A and 3B). Accumulation of DRiPs inside SGs was also observed when HSPA1A was depleted from cells (Figure 3C). We define these DRiP-enriched SGs, which show delayed disassembly

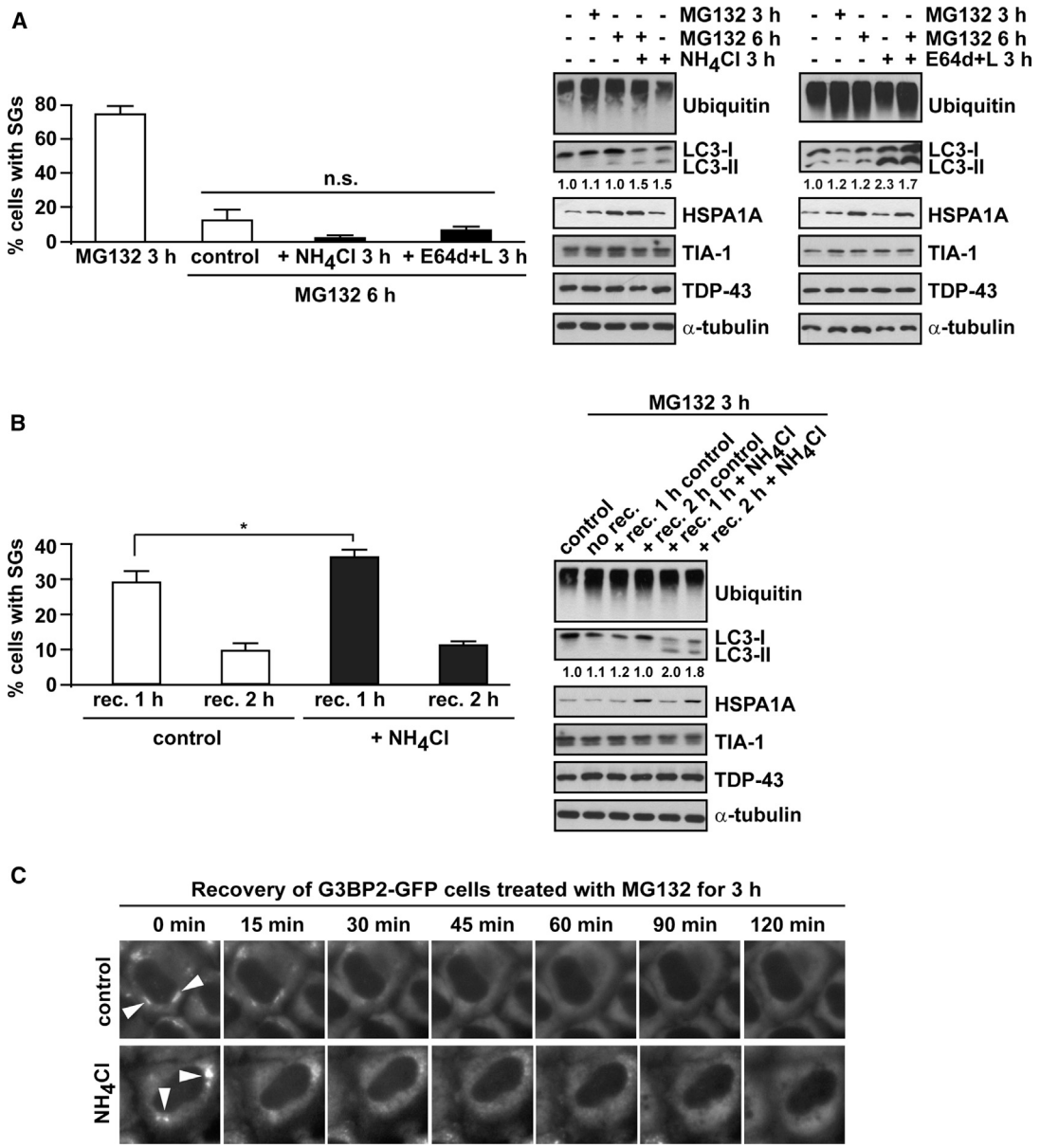

Figure 2. The Majority of SGs Disassemble Despite Inhibition of Autophagy

(A) Quantitation of percentage of HeLa cells with SGs after treatment with MG132 alone or with NH_4Cl 20 mM or E64d, 10 μg/ml, and leupeptin 200 μM for the indicated time points (n = 3–6) and western blot on total protein extracts. n.s., not significant. LC3-II/LC3-I ratio is shown.

(B) Cells were treated with MG132 for 3 hr and allowed to recover in absence or presence of NH_4Cl for 1 or 2 hr. Quantitation of % of cells with SGs (n = 3–7, ± SEM; *$p < 0.05$) and western blot on total protein extracts. LC3-II/LC3-I ratio is shown.

(C) Disassembly of SGs induced by MG132 treatment in G3BP2-GFP HeLa cells during the recovery in absence or presence of NH_4Cl.

See also Figure S2 and Movie S1.

kinetics (see Figure 1), as "aberrant" SGs. Importantly, in cells recovering from stress, aberrant SGs were particularly abundant (Figures 3D and 3E), suggesting that the presence of DRiPs leads to SG persistence.

A recent study proposed that SGs are composed of an RNase resistant core, which is maintained by protein-protein interactions and surrounded by an RNase-sensitive liquid-like shell (Jain et al., 2016). Thus, we hypothesized that core formation could be induced through the accumulation of DRiPs in SGs. To test this hypothesis, SGs were induced using MG132 and puromycin in the presence or absence of VER. At 3 hr after treatment, when the SG response was maximal, the cells were fixed or subjected to RNase treatment for 30 min. Staining of total RNA with SYTO RNASelect confirmed that the RNase significantly depleted RNA from the cytoplasm (Figure S2D). Remarkably, RNase treatment affected the number and size of SGs in control

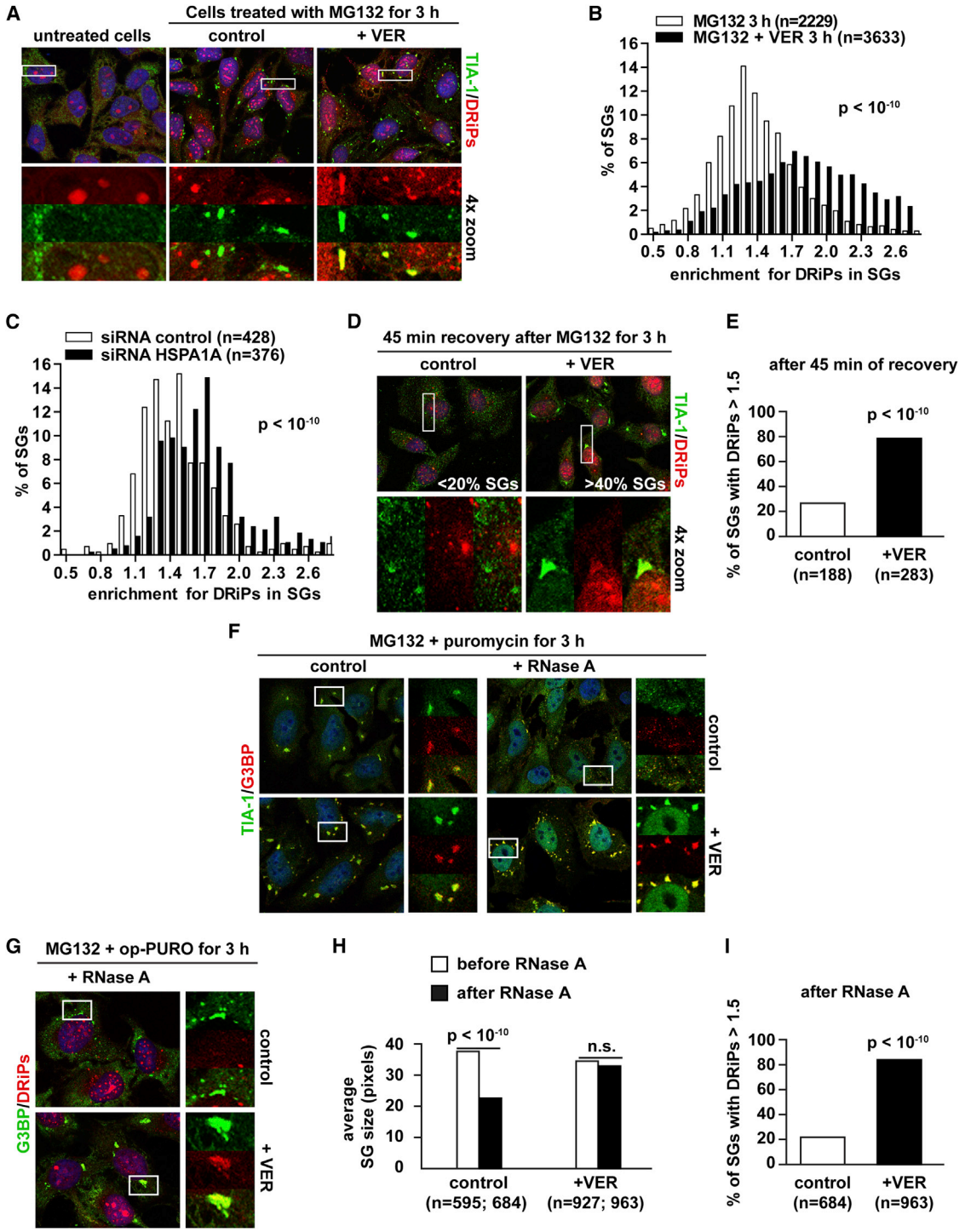

Figure 3. Inhibition of HSP70 Results in the Accumulation of DRiPs inside SGs

(A) SGs were induced in HeLa cells with MG132 alone or with VER for 3 hr, while labeling DRiPs with op-PURO 25 μM. TIA-1 SGs and DRiPs were visualized by microscopy.

(B) Quantitation of DRiP enrichment in SGs. $p < 10^{-10}$. Automated imaging and SG segmentation is based on TIA-1 signal. Data are presented as histogram.

(C) Quantitation of DRiP enrichment in SGs of control and HSPA1A-depleted cells. $p < 10^{-10}$. Data are presented as histogram.

(D) SGs were induced as described in (A). Where indicated, cells were allowed to recover for 45 min in absence or presence of VER. TIA-1 SGs and DRiPs were visualized by microscopy.

(E) Quantitation of DRiP enrichment in SGs from D. $p < 10^{-10}$. % of SGs enriched for DRiPs > 1.5 is shown.

(legend continued on next page)

cells, while it had no effect on SGs induced in cells treated with VER (Figure 3F). We next asked if these RNase-resistant SGs were enriched for DRiPs. Indeed, the SGs remaining after RNase treatment in VER-treated cells were strongly enriched for DRiPs compared to the control (Figures 3G–3I). This suggests a model in which the RNA-based interactions of SGs are progressively replaced by protein-protein interactions, which are mediated by DRiPs.

Combined, these data support the idea that chaperones prevent DRiP accumulation inside SGs, thereby maintaining their dynamics. From this point on, we will refer to this chaperone-mediated process of SG quality control that maintains SG dynamics and composition as "granulostasis."

The HSPB8-BAG3 Complex Cooperates with HSP70 to Mediate SG Disassembly

HSP70 cooperates with chaperones and co-chaperones, including the BAG family of proteins (BAG1–6). BAG proteins are nucleotide exchange factors that interact with the ATPase domain of HSP70. This interaction provides functional specificity to HSP70. For example, targeting bound substrates for degradation via the proteasome requires BAG1, whereas degradation via autophagy depends on BAG3 (Carra et al., 2008; Demand et al., 2001; Lüders et al., 2000). BAG3 forms a complex with HSP70 and HSPB8. HSPB8-BAG3-HSP70 is upregulated upon proteasome inhibition (Crippa et al., 2010) and targets (poly) ubiquitinated substrates (including DRiPs) for degradation (Minoia et al., 2014). This raised the question of whether HSP70 also cooperates with HSPB8 and BAG3 in the clearance of DRiPs from SGs and in the maintenance of SG dynamics.

To investigate this, we tested if these chaperones are recruited to SGs or, alternatively, to deposition sites that contain DRiPs and p62/SQSTM1, an autophagy receptor and marker for misfolded ubiquitinated proteins. We previously reported that BAG3 and HSP70 colocalize with SQSTM1-positive deposition sites, which are distinct from SGs (Minoia et al., 2014). Here, we find that HSPB8 does not colocalize with SQSTM1-containing sites but is recruited to TIA-1-positive SGs upon treatment with MG132 or arsenite (Figures 4A and S2E). In contrast, BAG3 did not colocalize with the majority of TIA-1 positive SGs under the same conditions (Figure 4A), suggesting that HSPB8 initially dissociates from BAG3-HSP70 to fulfil different functions. In agreement, HSP70 was also generally absent from arsenite or MG132-induced SGs (Figure S2F). Consistent with the absence of BAG3 from SGs, we found a strong colocalization of BAG3 with DRiP-containing deposition sites (Figure 4B). Importantly, HSPB8 was specifically recruited into SGs in cells exposed to proteotoxic stress (Figure 4C, arrowheads), but in unstressed cells, it colocalized with DRiP-containing sites (Figure 4C). We then performed co-immunoprecipitation experiments, which revealed that the amount of BAG3 co-immunoprecipitating with HSPB8 was indeed much lower in MG132-treated cells than in control cells (Figure S2G). Thus, the HSPB8-BAG3-HSP70 complex (partly) dissociates upon proteotoxic stress, and HSPB8 and BAG3-HSP70 are targeted to different locations.

Small HSPs often function as holdases, chaperones that bind misfolded proteins and present the bound client to HSP70 for refolding or targeting to degradation (Lee and Vierling, 2000). Consistent with the idea that HSPB8 presents misfolded substrates to HSP70 for further processing, we found that DRiP-containing SGs recruit increasing amounts of HSPB8 when HSP70 is inhibited with VER (Figure 4D). To test whether HSPB8 functions as a holdase inside SGs, we overexpressed mCherry-Ubc9TS, a misfolding-prone protein that co-aggregates with heat-induced SGs (D.M. and S.A., unpublished observations). SGs enriched for misfolded Ubc9TS recruited HSPB8 quantitatively. As a control, the amount of eIF3, a canonical SG component, did not correlate with the amount of Ubc9TS within SGs (Figure 4E). This suggests that HSPB8 functions as a chaperone inside SGs to prevent irreversible aggregation of misfolding-prone proteins, such as DRiPs.

Based on these findings, we reasoned that depletion of HSPB8 itself or of BAG3 (which stabilizes HSPB8) could impair SG disassembly. First, we confirmed that neither overexpression of HSPB8 or BAG3 (Figures S3A–S3D), nor downregulation of endogenous HSPB8 or BAG3 (Figures S3E–S3I; Movie S2) affects normal SG assembly. Next, we determined the percentage of cells with persistent SGs after prolonged MG132 treatment. Indeed, depletion of HSPB8 and BAG3 significantly increased the fraction of cells containing persistent SGs (Figures 5AC), similar to what was observed in HSPA1A-depleted cells (Figures 1A and S1D). Consistent with SG persistence, translation restoration was delayed in HSPB8- and BAG3-depleted cells (Figure 5D; Figure S4A). HSP70 was still induced upon prolonged treatment with MG132 in BAG3- and HSPB8-depleted cells (Figure S4A), suggesting that HSP70 cannot act independently of BAG3 or HSPB8 in SG disassembly. In contrast, induction of HSPB8 was dependent on the presence of BAG3 and vice versa (Figure S4B). This demonstrates that upregulation of both the HSPB8-BAG3 subcomplex and HSP70 are required to ensure SG disassembly and translation restoration upon prolonged proteasome inhibition.

We next looked at SG disassembly in BAG3- and HSPB8-depleted cells after MG132 removal, using fixed samples (Figures 5E and 5F) and live cell imaging (Figure S4C; Movie S3). Again, SGs exhibited delayed disassembly in BAG3- and HSPB8-depleted cells. Finally, we tested if depletion of BAG3 also leads to SG persistence after exposure to heat shock. The induction of SGs by temperature-upshift was not affected by

(F) SGs were induced in cells with MG132 and puromycin 5 μg/ml alone or with VER. After 3 hr, cells were fixed or permeabilized with Triton X-100 and incubated for 30 min in absence or presence of RNase A 0.2 mg/ml. Representative images of TIA-1 and G3BP SGs before and after RNase A treatment are shown.
(G) SGs were induced in cells with MG132 alone or with VER for 3 hr, while labeling DRiPs with op-PURO. After 3 hr, cells were fixed or subjected to RNase treatment as described in (F). G3BP SGs and DRiPs were visualized after RNase treatment by microscopy.
(H) Quantitation of average SG size (pixels) before and after RNase treatment in cells from (G). $p < 10^{-10}$. n.s. = not significant.
(I) Quantitation of DRiP enrichment in SGs before and after RNase treatment in cells from (G). $p < 10^{-10}$. % of SGs enriched for DRiPs > 1.5 is shown.
See also Figure S2.

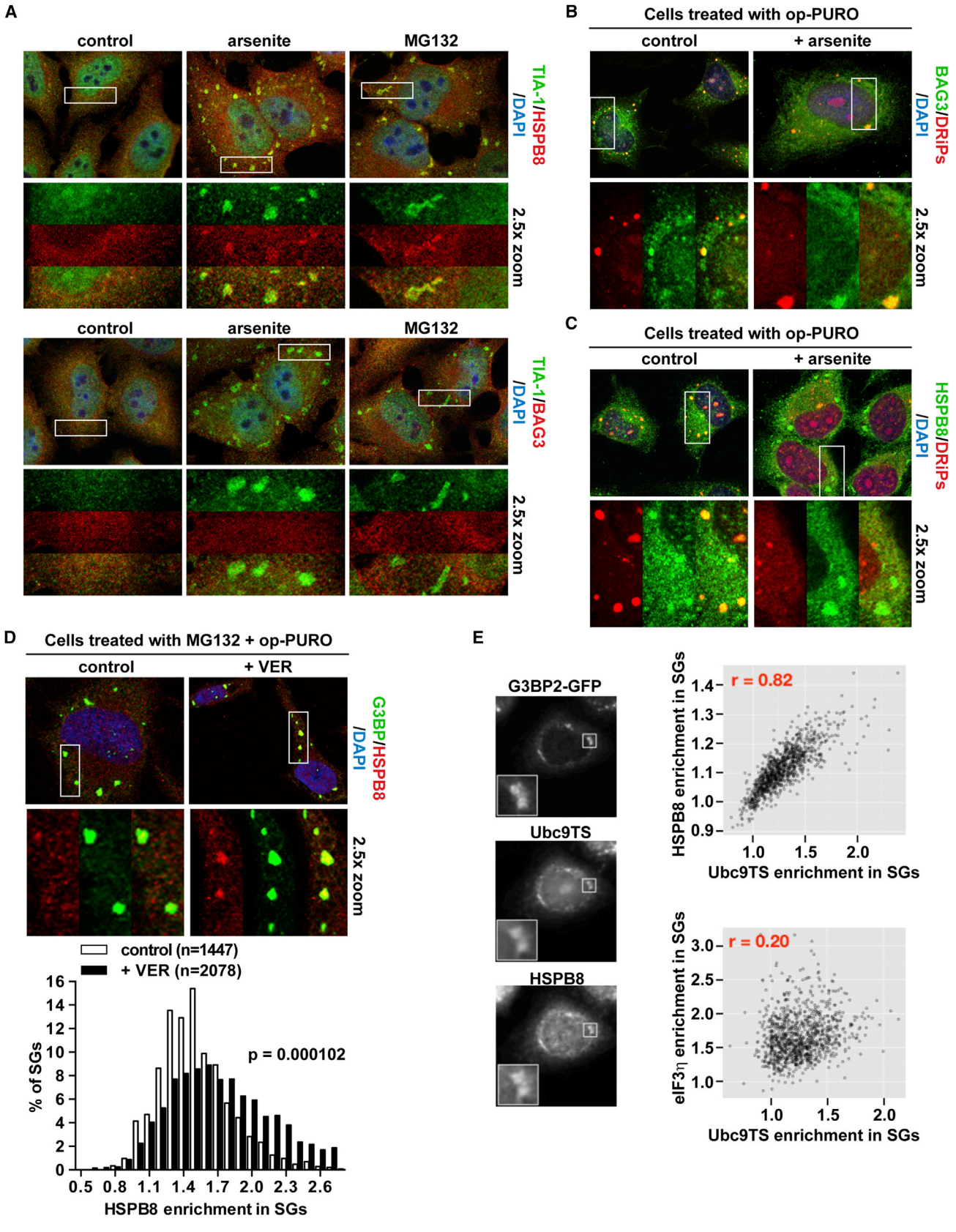

(legend on next page)

BAG3 depletion (Figure S4D), while SG disassembly was significantly delayed (Figure S4D; Movie S4). Thus, we conclude that HSPB8-BAG3-HSP70 ensures SG disassembly under different proteotoxic stresses.

HSPB8 Neutralizes Misfolded Proteins in Aberrant SGs and Recruits BAG3 and HSP70

We sought to determine if delayed SG disassembly in HSPB8-BAG3-depleted cells correlates with DRiP retention within SGs. Despite incomplete depletion of HSPB8 or BAG3 using siRNA (Figure S3E), we observed a significant retention of DRiPs inside SGs (Figure 6A). We next evaluated the sensitivity of SGs to RNase. Before RNase treatment SGs had similar size in all conditions tested (Figures 6B and 6C). After RNase treatment, the average size of SGs was significantly reduced in control cells, whereas no effect was observed in BAG3-depleted cells (Figures 6B and 6C). Combined with the increased recruitment of HSPB8 into SGs that contain mCherry-Ubc9TS (Figure 4E), these data suggest that HSPB8 acts as chaperone inside SGs to prevent irreversible aggregation of misfolded proteins and DRiPs, which may subsequently be transferred to BAG3-HSP70 to be targeted for degradation.

We next investigated if depletion of BAG3 (that destabilizes HSPB8) affects the cells' ability to clear accumulated DRiPs. The overall amount of DRiPs was significantly increased in BAG3-depleted cells (Figure 6D; Figure S4E), suggesting that BAG3-HSPB8 is required for DRiP removal. Next, we tested whether HSPB8 in aberrant SGs promotes the transfer of misfolded clients to BAG3-HSP70. Indeed, aberrant DRiP-containing SGs heavily recruited BAG3 (Figures 6E and 6F). These BAG3-containing SGs were large in size and often located in an area close to the nuclear envelope (data not shown). Both inhibition of HSP70 with VER or genetic depletion of HSPA1A increased BAG3 recruitment into aberrant SGs (Figures 6F and 6G). In contrast, depletion of HSPB8 did not have such an effect but rather reduced BAG3 recruitment into aberrant SGs (Figure 6G). This is consistent with a model in which HSPB8 recruits BAG3 into aberrant SGs.

Previous reports showed that misfolded proteins accumulate in the perinuclear region to be degraded via autophagy or stored in the aggresome (Iwata et al., 2005). Thus, we tested whether recovering cells contain high amounts of perinuclear DRiPs. Indeed, after prolonged treatment with MG132, when the majority of SGs have disassembled (Figures 1A and 2A), DRiPs localized in clusters close to the nuclear envelope (Figure S4F). These juxtanuclear DRiP aggregates contained high amounts of HSPB8 and BAG3 (Figure S4F). Thus, we conclude that granulostasis by HSPB8-BAG3-HSP70 is a two-step process. First, HSPB8 accumulates in SGs and maintains misfolded proteins in a competent state for further processing, preventing their irreversible aggregation inside SGs. Second, HSPB8 recruits BAG3-HSP70 to extract misfolded proteins, which subsequently accumulate in the perinuclear region where they are targeted for degradation by autophagy.

Other Proteins Cannot Functionally Replace BAG3, HSPB8, and HSPA1A in Granulostasis

Depletion of BAG3, HSPB8, or HSPA1A affects SG properties. To exclude that this is due to an indirect effect caused by general impairment of proteostasis, we investigated BAG1 and HSPB1, other members of the BAG or small HSP families. In HeLa cells, BAG1 was not recruited into SGs induced by arsenite or MG132 (Figure S5A). Moreover, BAG1 depletion did not affect SG assembly or disassembly (Figure S5B), nor did it influence the translation rate or the expression of BAG3 and its partners HSPB8 and HSP70 (Figure S5C). SGs forming in BAG1-depleted cells were also not enriched for DRiPs (Figure S5D). Concerning HSPB1, we found that in contrast to HSPB8, HSPB1 was not generally recruited into arsenite or MG132-induced SGs (Figure S6A). However, aberrant SGs containing DRIPs significantly recruited HSPB1 (Figure S6A; MG132 + VER for 3 hr). In agreement, we found a mild delay in SG disassembly in HSPB1-depleted cells upon prolonged treatment with MG132 (Figures S6B and S6C). This correlated with a moderate increase in the amount of DRiPs inside SGs in HSPB1-depleted cells (Figure S6D). This suggests that HSPB1 assists in the quality control of SGs and is in line with a study that reported enrichment of HSPB1 in heat-induced SGs (Jain et al., 2016). However, in contrast to HSPB8, HSPB1 is recruited with a significant delay into SGs, suggesting that it functions in the late phase when SGs have accumulated high amounts of misfolded proteins. Altogether, these data suggest a specific role for BAG3-HSPB8-HSP70 in SG quality control.

HSPB8-BAG3-HSP70 Promotes Disassembly of SGs Containing Mutant RBPs

FUS and hnRNPA1 form liquid droplets that convert with time into hydrogels or fibers. This is accelerated by disease mutations in *FUS* or *hnRNPA1* (Molliex et al., 2015; Patel et al., 2015). Thus, we asked if aberrant SGs that contain mutated RBPs are subject to protein quality control by HSPB8-BAG3-HSP70.

We used HeLa cells expressing GFP-tagged wild-type (WT) FUS or the ALS-associated mutant G156E to study SG disassembly or clearance (Patel et al., 2015). As before, we induced SGs by MG132 treatment and allowed the cells to recover for 3 hr in absence or presence of NH_4Cl. Inhibition of lysosomes,

Figure 4. SGs Recruit HSPB8

(A) Immunofluorescence on HeLa cells untreated or exposed to arsenite (0.5 mM) for 45 min or MG132 for 3 hr to visualize HSPB8 or BAG3 recruitment into TIA-1 SGs.

(B and C) Staining of DRiPs, HSPB8, and BAG3 in cells treated for 45 min with op-PURO alone or with arsenite.

(D) Immunofluorescence on cells treated for 3 hr with MG132 and op-PURO alone (control) or with VER. Quantitation of HSPB8 enrichment in G3BP SGs. $p = 0.000102$. Automated imaging and SG segmentation is based on G3BP signal.

(E) Enrichment of eIF3η (used as control), HSPB8, and Ubc9ts-mCherry in SGs in G3BP2-GFP HeLa cells exposed to heat at 43°C for 2 hr. Automated imaging and SG segmentation is based on G3BP2-GFP signal. Pearson's correlation coefficient (r) is shown.

See also Figure S2.

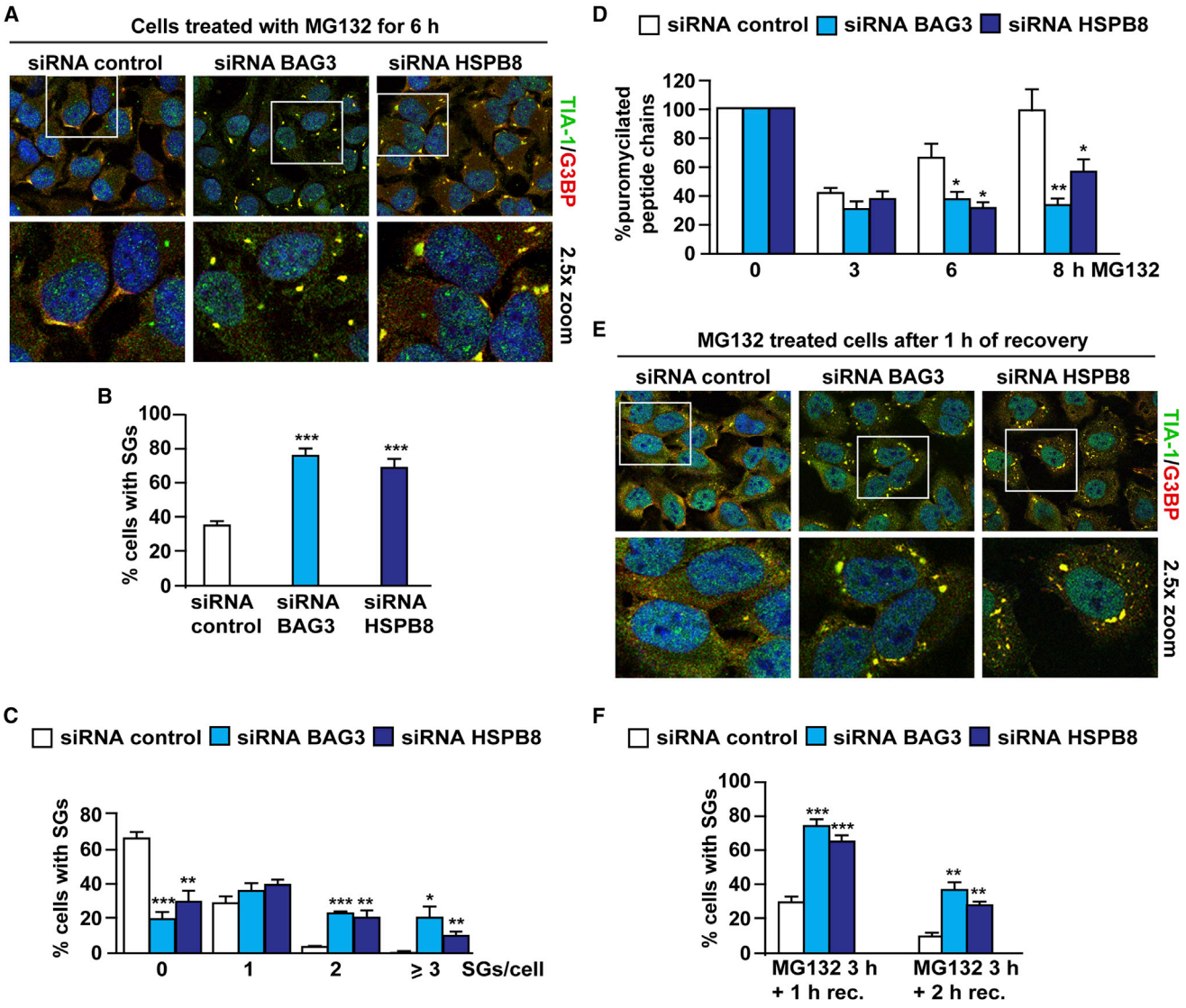

Figure 5. Depletion of HSPB8 and BAG3 Delays SG Disassembly

(A) SG disassembly in HeLa cells lipofected with BAG3, HSPB8, or nontargeting control siRNA for 72 hr and treated with MG132 for 6 hr.

(B) Quantitation of percentage of cells with SGs. n = 3–5, ± SEM; ***p < 0.001.

(C) Quantitation of the number of SGs/cell. n = 3–5, ± SEM; *p < 0.05; **p < 0.01; ***p < 0.001.

(D) Quantitation of puromycin incorporation in control or in BAG3- or HSPB8-depleted cells after treatment with MG132 for the indicated time points. Puromycin 5 μg/ml was added during the last 15 min of treatment, prior to protein extraction. n = 3–4, ± SEM; *p < 0.05; **p < 0.01.

(E) TIA-1 and G3BP immunofluorescence to visualize SGs in control and in HSPB8- or BAG3-depleted HeLa cells treated for 3 hr with MG132 and allowed to recover for 1 or 2 hr in drug-free medium.

(F) Quantitation of percentage of cells with persisting SGs. n = 3–5, ± SEM; **p < 0.01; ***p < 0.001.

See Figures S3 and S4 and Movies S2, S3, and S4.

which led to LC3-II accumulation (Figure 7A, right), did not cause the persistence of SGs containing WT or G156E FUS (Figure 7A, left). Next, we induced SGs in both cell lines with MG132 and allowed the cells to recover overnight in the presence of proteasome or lysosome inhibitors (Figure S7A). Again, nearly all cells disassembled the pre-formed SGs (Figure 7B). To confirm that lysosome inhibition was effective, we performed an immunofluorescence staining with an anti-SQSTM1 antibody. SQSTM1 positive structures were present in all cells, with SQSTM1 accumulating at the microtubule-organizing center (MTOC) and forming a structure that resembles the aggresome (Figure 7B). After overnight inhibition of lysosomes, only a few cells (fewer than 1%) contained persisting SGs. These persisting SGs contained high amounts of BAG3 (Figure 7C), suggesting that they were subject to quality control by HSPB8-BAG3-HSP70. This demonstrates that SGs containing WT or mutant G156E FUS are treated

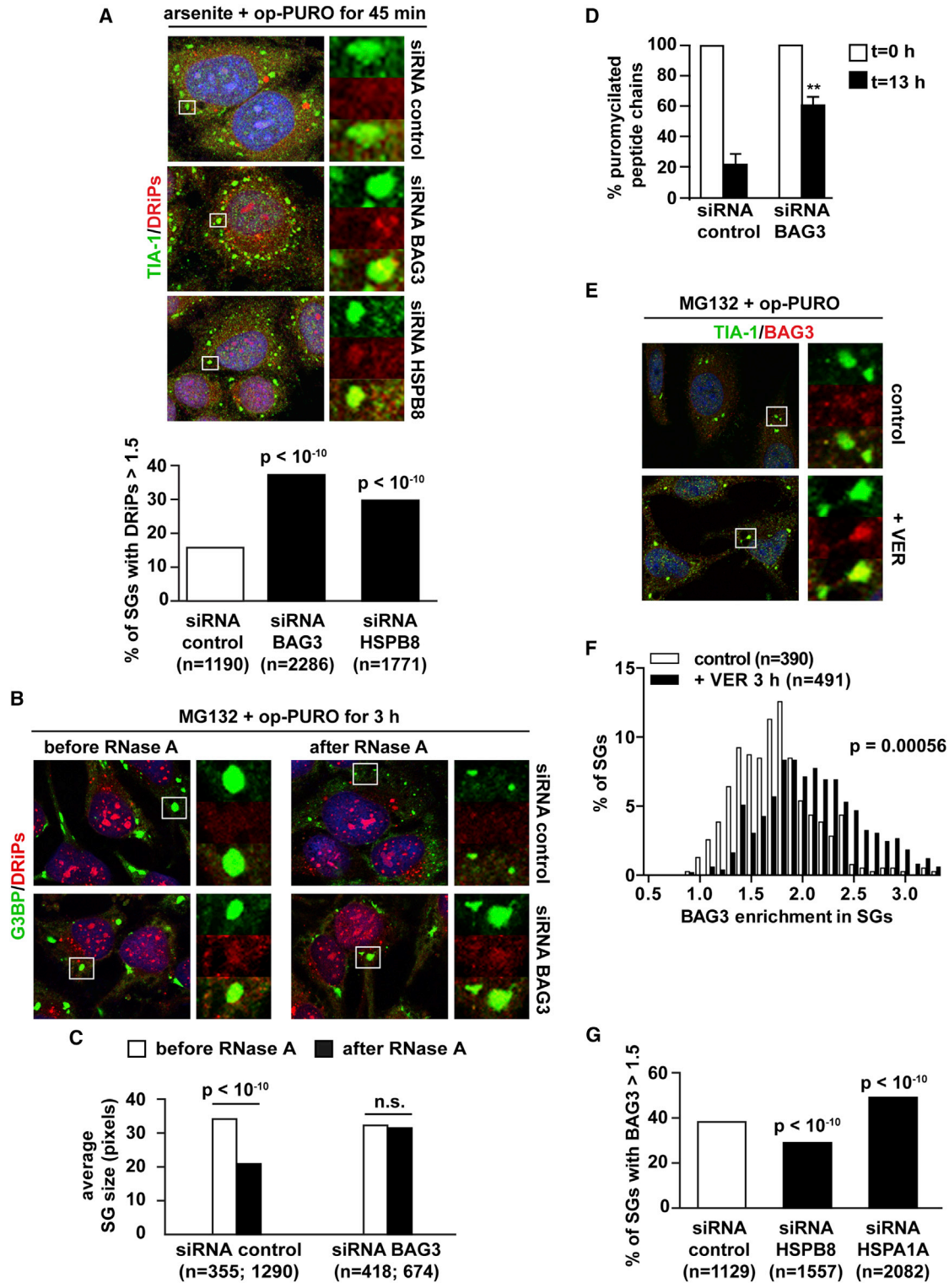

Figure 6. HSPB8-BAG3 Prevents the Accumulation of DRiPs in SGs

(A) TIA-1 and DRiPs immunofluorescence in control and in BAG3- or HSPB8-depleted HeLa cells co-treated with arsenite and op-PURO for 45 min. Quantitation of DRiP enrichment in SGs. $p < 10^{-10}$. % of SGs enriched for DRiPs > 1.5 is shown.

(B) SGs were induced in control or BAG3-depleted cells by treatment with MG132 for 3 hr, while labeling DRiPs with op-PURO. After 3 hr, cells were fixed (before RNase A) or treated with RNase A (after RNase A). G3BP SGs and DRiPs were visualized by fluorescence microscopy before and after RNase treatment.

(legend continued on next page)

similarly and that cells generally prefer to disassemble SGs rather than target them to autophagy for degradation.

We next tested if depletion of BAG3 leads to persisting SGs in cells expressing WT or G156E FUS. Depletion of BAG3 per se did not change the expression level of the *FUS* transgenes (Figure S7B). We next exposed cells to 6 hr of MG132 and determined the number of remaining SGs. The percentage of cells with persisting SGs was significantly higher for G156E than for WT FUS, showing that the ALS-associated mutation affects SG disassembly (Figure 7D). Depletion of BAG3 significantly delayed SG disassembly in both cell lines (Figures 7D, S7C, and S7D). This indicates that G156E SGs cannot efficiently be disassembled when cells are exposed to prolonged proteasome inhibition and that the persisting G156E SGs are subject to control by the granulostasis machinery.

We next exposed cells expressing G156E FUS to prolonged treatment with MG132 to determine the fate of DRiPs and granulostasis factors when misfolded proteins cannot be degraded by the proteasome. Under these conditions, DRiPs accumulated at or nearby the MTOC in aggresome-like structures together with SQSTM1 (Figure S7E) and HSPB8-BAG3 (Figure S4F). In contrast, G156E FUS did not colocalize with SQSTM1 at the aggresome (Figure 7E). This indicates that SGs containing G156E FUS can be disassembled and that G156E FUS is not recognized as a severely misfolded protein and is not generally targeted to the aggresome for degradation. This also suggests that the granulostasis machinery can extract DRiPs from SGs containing mutant RBPs, and that these DRiPs are targeted to the aggresome when they cannot be degraded.

We next investigated if the slower disassembly of G156E SGs is due to accumulation of DRiPs. Indeed, SGs containing G156E FUS entrap higher amounts of DRiPs than SGs containing wild-type FUS (Figure 7F). Interestingly, during prolonged treatment with MG132, SGs that failed to disassemble became progressively more enriched for DRiPs (Figure 7F, lower panel; compare 3 and 6 hr), supporting the interpretation that co-aggregation of SGs with DRiPs changes their dynamics. This effect was more pronounced for SGs containing G156E FUS, suggesting that there may be direct interactions between DRiPs and mutated proteins, such as G156E FUS in SGs. A cross-talk between misfolded proteins and mutant RBPs is further supported by our finding that aberrant SGs in fibroblasts from an ALS patient carrying a mutation in TDP-43 (G294V) (Del Bo et al., 2009) recruit BAG3 more strongly than SGs in control fibroblasts (Figure S7F) and entrap higher amounts of DRiPs (Figure 7G). Furthermore, DRiP enrichment in SGs containing G294V TDP-43 correlated with delayed disassembly when compared with SGs containing WT TDP-43 (Figure 7H). Thus, we conclude that mutant RBPs can affect SG dynamics in part due to intrinsic properties of the mutant protein itself and in part due to increased retention of DRiPs inside SGs. As a consequence, aberrant SGs containing mutant RBPs and DRiPs have an increased dependence on HSPB8-BAG3-HSP70 for disassembly.

DISCUSSION

Here, we show that in mammalian cells, when the PQC is impaired or in the presence of mutated RBPs, SGs have tendency to accumulate misfolded proteins, such as DRiPs, and then become aberrant and persist. We find that disassembly of these aberrant SGs relies on an active PQC system that surveys SG composition and ensures SG dynamics. This, in turn, allows translation restoration when the stress subsides. We refer to this SG surveillance function of the PQC system as granulostasis.

We previously reported that SGs are generally devoid of aggregated DRiPs, which can accumulate within SGs when autophagy is impaired (Seguin et al., 2014). Here, we demonstrate that, when a specific chaperone-mediated disposal mechanism is compromised, misfolded proteins and DRiPs accumulate inside SGs, thereby altering SG biochemistry and dynamics and causing defects in SG disassembly. We identify the HSPB8-BAG3-HSP70 chaperone complex as a key player of granulostasis. The incidence of aberrant DRiP-containing SGs under normal conditions is very low, suggesting that the protein quality control machinery is highly efficient in preventing aberrant SG formation.

We were surprised to find that, immediately after stress, HSPB8 dissociates from the BAG3-HSP70 subcomplex and is specifically recruited into SGs (Figure 4). BAG3 and HSP70 are not recruited into SGs upon arsenite or MG132 treatment, but colocalize with DRiPs in cytosolic aggregates that also contain SQSTM1. Once inside SGs, HSPB8 seems to act as an ATP-independent chaperone "holder" that neutralizes misfolded proteins (Ubc9TS) and DRiPs. In fact, the amount of HSPB8 and misfolded proteins inside SGs strongly correlate (Figure 4). The fast recruitment kinetics of HSPB8, coupled with the fact that HSPB8 is an intrinsically disordered protein (Sudnitsyna et al., 2012), suggest that dissociated HSPB8 has a high affinity for phase-separated SGs and may increasingly be retained inside SGs when it encounters misfolded proteins. In fact, an emerging theme suggests that many proteins that partition into membrane-less liquid-like compartments have extended regions of intrinsic disorder (Brangwynne et al., 2015; Gilks et al., 2004; Patel et al., 2015).

Once inside SGs, HSPB8 recruits BAG3 to promote client transfer and processing by the BAG3-HSP70 machinery (Figure 6). Although HSPB8 binds to misfolded substrates to prevent their irreversible aggregation, it cannot itself refold or target

(C) Quantitation of SG size (pixels) before and after RNase treatment in cells from B. $p < 10^{-10}$. n.s. = not significant.
(D) Quantitation of puromycilated proteins in control or BAG3-depleted cells treated with arsenite and puromycin 10 μg/ml for 45 min and allowed to recover for 13 hr in drug-free medium. n = 3/condition, ± SEM; $^{**}p < 0.01$.
(E) TIA-1 and BAG3 immunofluorescence and quantitation of BAG3 recruitment in SGs induced with MG132 and op-PURO alone or with VER for 3 hr.
(F) Quantitation of BAG3 enrichment in SGs in cells treated as described in E. $p = 0.00056$. Data are presented as histogram.
(G) Quantitation of BAG3 enrichment in SGs induced with MG132 and VER in control and in HSPB8- or HSPA1A-depleted cells. $p < 10^{-10}$. Percentage of SGs with DRiP enrichment > 1.5 is shown.
See also Figures S4–S6.

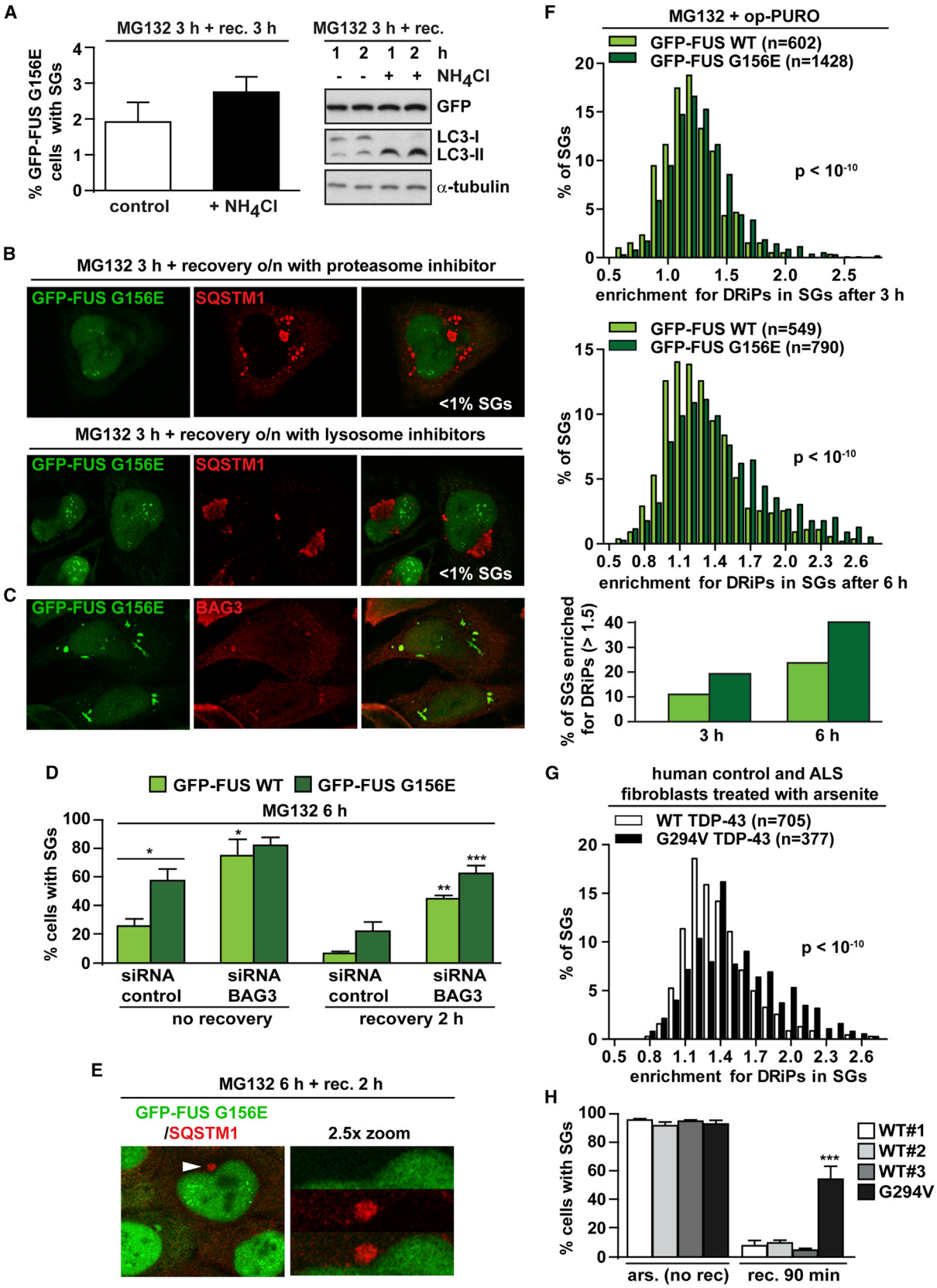

(legend on next page)

bound substrates to degradation (Carra et al., 2005). Their fate depends on HSPB8-dependent recruitment of BAG3 (Carra et al., 2008). Indeed, association of BAG3 with SQSTM1 targets HSPB8-BAG3-HSP70 bound clients to autophagy (Crippa et al., 2010; Gamerdinger et al., 2011). Thus, we propose that HSPB8 is recruited to SGs to maintain DRiPs (and other misfolding-prone proteins) in a competent state for efficient transfer to BAG3-HSP70. The neutralization of DRiPs inside SGs by HSPB8 and the timely sorting by BAG3-HSPB8 of DRiPs into perinuclear aggregates that are spatially separated from SGs are crucial to maintain SG composition and dynamics (granulostasis). In agreement with this, even a moderate depletion of BAG3-HSPB8 causes a conversion of SGs into an aberrant, RNase-resistant state (Figure 6).

We can also envision that, once inside SGs, HSPB8 prevents the irreversible aggregation of RBPs with aggregation-prone low complexity domains. However, the finding that depletion of HSPB8 is sufficient to cause retention of DRiPs inside SGs, despite the fact that HSP70 is functional and some BAG3 is still present (Figure 6), points to a key role of HSPB8 in maintaining DRiPs in a competent state for sorting and processing. This may be either by directly acting on DRiPs or by preventing promiscuous interactions between DRiPs and RBPs or both. A similar function may be exerted by HSPB1, another small HSP that holds misfolded proteins for transfer to HSP70 (Bryantsev et al., 2007). In contrast to HSPB8, which is immediately recruited into forming SGs, HSPB1 is only detected in aberrant SGs, suggesting that it is an important player in a second line of defense.

When the stress subsides and SGs disassemble, HSPB8, BAG3-HSP70, and SQSTM1 all colocalize with DRiPs that accumulate at the aggresome (Figures S4F and S7E). This observation supports the notion that HSPB8-BAG3-HSP70 actively extracts DRiPs from aberrant SGs. We do not know how misfolded proteins are extracted from aberrant SGs, but we suspect that ATP-driven cycling of HSP70 may provide a pulling force for misfolded protein removal. If the misfolded proteins cannot be efficiently degraded after extraction, for example because of the inhibition of autophagy, cells activate an alternative pathway to deposit misfolded proteins at the aggresome. This suggests that cells avoid the degradation of entire SGs but prefer to disassemble aberrant SGs into their components, and then only target the misfolded proteins for degradation. Indeed, in contrast to DRiPs, most SG components, including mutated G156E FUS, will be released from SGs and do not accumulate with SQSMT1 at the aggresome (Figure 7E). Thus, targeting to autophagy is not the preferred pathway for SG components such as FUS.

Despite the fact that G156E FUS was not recognized as a granulostasis substrate, G156E FUS conferred aberrant dynamics to SGs. SGs containing G156E FUS accumulated significantly higher amounts of DRiPs as WT FUS SGs, supporting the conclusion of a cross-talk between mutated RBPs and DRiPs. A higher propensity of G156E SGs to convert into a solid state could lead to increased retention of further aggregation-prone DRiPs in SGs, an idea that is supported by observations in fALS fibroblasts with a mutation in TDP-43 (G294V; Figure 7G). Consistent with this, G156E SGs depend on a functional HSPB8-BAG3-HSP70 complex for disassembly. These results demonstrate that chaperone-assisted SG disassembly is the preferred pathway adopted by the majority of SGs. This does not exclude that extensive co-aggregation of SGs with misfolded proteins triggers a partial or complete digestion of SGs via autophagy. Indeed, we noticed some colocalization of FUS G156E with SQSTM1 in BAG3-depleted cells, supporting that, when disassembly fails, components of aberrant RNP assemblies can be targeted for autophagy. Combined, our data indicate that, in ALS, mechanisms other than autophagy must fail on the path to a full-blown disease, which is supported by genetic evidence (Robberecht and Philips, 2013).

Genetic mutations associated with ALS and related diseases can be placed into two groups. In the first group, there are mutations in misfolding-prone proteins, such as SOD1, or mutations in PQC factors, such as VCP, SQSTM1, or optineurin (Robberecht and Philips, 2013). In the second group, there are mutations in RBP components of SGs, which generally seem to increase the aggregation propensity of these RBPs. It is still unclear if these two groups of factors function in the same or distinct pathways of the disease. Our data suggest a model in which these two sets of factors converge on a common pathway. Both groups of factors share the ability to modify the properties and compositions of RNP granules and determine if these compartments remain dynamic or turn into dysfunctional aggregates. This suggests that, at the core of such diseases as ALS may be a failure to maintain RNP granules in a dynamic, liquid-like state because of aberrant interactions between misfolded

Figure 7. BAG3 Is Recruited into SGs Containing Mutated *FUS* to Assist Their Disassembly

(A) GFP-FUS G156E HeLa cells treated with MG132 for 3 hr and allowed to recover in absence or presence of NH_4Cl for 3 hr. Quantitation of percentage of cells with SGs (left). n = 3/condition. Western blot on protein extracts (right).

(B and C) GFP and SQSMT1 (B) or BAG3 (C) immunofluorescence on GFP-FUS G156E HeLa cells treated with MG132 for 3 hr and allowed to recover overnight in presence of bortezomib 100 nM, a proteasome inhibitor, or E64d and leupeptin, lysosome inhibitors.

(D) Quantitation of SGs in GFP-FUS WT or G156E HeLa cells lipofected with BAG3 or nontargeting control siRNA and treated with MG132 for 6 hr. n = 3/condition, ± SEM; **p < 0.01; ***p < 0.001.

(E) GFP and SQSMT1 immunofluorescence in GFP-FUS G156E HeLa cells treated with MG132 for 6 hr and allowed to recover for 2 hr in drug-free medium.

(F) Quantitation of DRiP enrichment in SGs in GFP-FUS WT or G156E HeLa cells treated with MG132 for 3 or 6 hr. $p < 10^{-10}$. Data are presented as histograms.

(G) Quantitation of DRiP enrichment in SGs in fibroblasts from three healthy participants and from one fALS patient with the TDP-43 G294V mutation exposed to arsenite for 45 min prior to fixation. $p < 10^{-10}$. Data are presented as histogram.

(H) SGs in fibroblasts from three healthy participants, WT#1–3, disassemble more rapidly than SGs in fibroblasts from one fALS patient with the TDP-43 G294V mutation. Cells were exposed to arsenite for 45 min and fixed or allowed to recover in drug-free medium for 90 min. Cells were stained for TIA-1 and G3BP. Percentage of cells with SGs was counted. n = 3/condition, ± SEM; ***p < 0.001.

See Figure S7.

proteins and aggregation-prone RBPs. In fact, the misfolding-prone proteins that may initiate a pathological state may directly be produced at the ribosome as DRiPs. This is supported by genetic evidence of a potential genetic link between ALS-like diseases and general ribosomal PQC (Chu et al., 2009).

Approaches aimed at inducing the expression of HSPB8, BAG3, and HSP70 should have a promising outcome in ALS models by acting at the level of proteostasis and granulostasis, ultimately ensuring proper translation restoration and RNA expression. Conversely, mutations of *HSPB8* and *BAG3* associated with motor neuropathy and muscular dystrophy may cause disease because of an impairment of granulostasis (Ghaoui et al., 2016; Irobi et al., 2004; Selcen et al., 2009). In fact, several proteins associated with motor neuron diseases, including HSPB1, have been identified as new components of SGs (Jain et al., 2016), further substantiating the notion that defective granulostasis may represent a key pathomechanism in motor neuron diseases.

EXPERIMENTAL PROCEDURES

Detailed methods are available in the Supplemental Information.

Ethics Statement

Protocols and informed consent were approved by the Institutional Ethics Committee (Protocol n°375/04, 07/01/2004).

Cell Lines

HeLa-Kyoto cells stably expressing G3BP2-GFP, GFP-FUS wild-type (WT) or G156E were previously described (Poser et al., 2008). HeLa HSPB8 and BAG3 Flp-In cells were produced using Flp-in System.

Stress, Inhibitor Treatment, and Labeling of Nascent Peptides with op-PURO

Cells were treated for the indicated time-points, immediately fixed or let to recover in growth medium (control) or in presence of inhibitors.

The protocol for op-PURO labeling was previously described (Seguin et al., 2014).

Immunofluorescence Microscopy and Live Cell-Imaging Analysis

Cells were fixed with 3.7% formaldehyde for 9 min at RT and permeabilized with acetone for 5 min at −20°C. Cells were analyzed using a confocal Leica SP2 system.

Live-imaging was done using the DeltaVision imaging system and softWorx 4.1.2.

RNase Sensitivity

After SG induction, cells were washed with PBS containing Triton X-100 (0.05%), followed by wash with PBS. Cells were incubated in growth medium with RNase A Solution (0.2 mg/ml) at RT for 30 min. Cells were fixed with formaldehyde or methanol prior to staining with antibodies, Alexa 594-Azide, or SYTO RNASelect (Seguin et al., 2014).

SUPPLEMENTAL INFORMATION

Supplemental Information includes Supplemental Experimental Procedures, seven figures, and four movies and can be found with this article online at http://dx.doi.org/10.1016/j.molcel.2016.07.021.

AUTHOR CONTRIBUTIONS

M.G., I.B., and L.M. performed the experiments. F.F.M. generated inducible cells. D.M. analyzed SG composition. J.V., S.J.S., and G.L. assisted with microscopy. I.P. constructed BAC cells. I.P. and H.L. assisted with live-imaging. O.P. and C.C. provided fibroblasts. A.P. assisted in paper writing. S.C. conceived the project. S.C. and S.A. developed the project and wrote the paper.

ACKNOWLEDGMENTS

We thank Dr. T. Franzmann and members of the MPI-CBG for manuscript critical reading. D.M. was supported by DFG-Center for Regenerative Therapies. S.C. and A.P. are grateful to AriSLA for funding. S.C. is grateful to MIUR and Ministry of Health for funding. S.A., S.C., and A.P. are grateful to the JPND network. This is an EU Joint Programme - Neurodegenerative Disease Research (JPND) project. The project is supported through funding organisations under the aegis of JPND (http://www.neurodegenerationresearch.eu/). This project has received funding from the European Union's Horizon 2020 Research and Innovation Programme under grant agreement No 643417.

Received: February 29, 2016
Revised: June 28, 2016
Accepted: July 20, 2016
Published: August 25, 2016

REFERENCES

Brangwynne, C.P., Tompa, P., and Pappu, R.V. (2015). Polymer physics of intracellular phase transitions. Nat. Phys. *11*, 899–904.

Bryantsev, A.L., Kurchashova, S.Y., Golyshev, S.A., Polyakov, V.Y., Wunderink, H.F., Kanon, B., Budagova, K.R., Kabakov, A.E., and Kampinga, H.H. (2007). Regulation of stress-induced intracellular sorting and chaperone function of Hsp27 (HspB1) in mammalian cells. Biochem. J. *407*, 407–417.

Buchan, J.R., Kolaitis, R.M., Taylor, J.P., and Parker, R. (2013). Eukaryotic stress granules are cleared by autophagy and Cdc48/VCP function. Cell *153*, 1461–1474.

Carra, S., Sivilotti, M., Chávez Zobel, A.T., Lambert, H., and Landry, J. (2005). HspB8, a small heat shock protein mutated in human neuromuscular disorders, has in vivo chaperone activity in cultured cells. Hum. Mol. Genet. *14*, 1659–1669.

Carra, S., Seguin, S.J., Lambert, H., and Landry, J. (2008). HspB8 chaperone activity toward poly(Q)-containing proteins depends on its association with Bag3, a stimulator of macroautophagy. J. Biol. Chem. *283*, 1437–1444.

Cherkasov, V., Hofmann, S., Druffel-Augustin, S., Mogk, A., Tyedmers, J., Stoecklin, G., and Bukau, B. (2013). Coordination of translational control and protein homeostasis during severe heat stress. Curr. Biol. *23*, 2452–2462.

Chu, J., Hong, N.A., Masuda, C.A., Jenkins, B.V., Nelms, K.A., Goodnow, C.C., Glynne, R.J., Wu, H., Masliah, E., Joazeiro, C.A., and Kay, S.A. (2009). A mouse forward genetics screen identifies LISTERIN as an E3 ubiquitin ligase involved in neurodegeneration. Proc. Natl. Acad. Sci. USA *106*, 2097–2103.

Crippa, V., Sau, D., Rusmini, P., Boncoraglio, A., Onesto, E., Bolzoni, E., Galbiati, M., Fontana, E., Marino, M., Carra, S., et al. (2010). The small heat shock protein B8 (HspB8) promotes autophagic removal of misfolded proteins involved in amyotrophic lateral sclerosis (ALS). Hum. Mol. Genet. *19*, 3440–3456.

Del Bo, R., Ghezzi, S., Corti, S., Pandolfo, M., Ranieri, M., Santoro, D., Ghione, I., Prelle, A., Orsetti, V., Mancuso, M., et al. (2009). TARDBP (TDP-43) sequence analysis in patients with familial and sporadic ALS: identification of two novel mutations. Eur. J. Neurol. *16*, 727–732.

Demand, J., Alberti, S., Patterson, C., and Höhfeld, J. (2001). Cooperation of a ubiquitin domain protein and an E3 ubiquitin ligase during chaperone/proteasome coupling. Curr. Biol. *11*, 1569–1577.

Gamerdinger, M., Kaya, A.M., Wolfrum, U., Clement, A.M., and Behl, C. (2011). BAG3 mediates chaperone-based aggresome-targeting and selective autophagy of misfolded proteins. EMBO Rep. *12*, 149–156.

Ghaoui, R., Palmio, J., Brewer, J., Lek, M., Needham, M., Evila, A., Hackman, P., Jonson, P.H., Penttila, S., Vihola, A., et al. (2016). Mutations in HSPB8

causing a new phenotype of distal myopathy and motor neuropathy. Neurology *86*, 391–398.

Gilks, N., Kedersha, N., Ayodele, M., Shen, L., Stoecklin, G., Dember, L.M., and Anderson, P. (2004). Stress granule assembly is mediated by prion-like aggregation of TIA-1. Mol. Biol. Cell *15*, 5383–5398.

Irobi, J., Van Impe, K., Seeman, P., Jordanova, A., Dierick, I., Verpoorten, N., Michalik, A., De Vriendt, E., Jacobs, A., Van Gerwen, V., et al. (2004). Hot-spot residue in small heat-shock protein 22 causes distal motor neuropathy. Nat. Genet. *36*, 597–601.

Iwata, A., Riley, B.E., Johnston, J.A., and Kopito, R.R. (2005). HDAC6 and microtubules are required for autophagic degradation of aggregated huntingtin. J. Biol. Chem. *280*, 40282–40292.

Jain, S., Wheeler, J.R., Walters, R.W., Agrawal, A., Barsic, A., and Parker, R. (2016). ATPase-Modulated stress granules contain a diverse proteome and substructure. Cell *164*, 487–498.

Kedersha, N., and Anderson, P. (2002). Stress granules: sites of mRNA triage that regulate mRNA stability and translatability. Biochem. Soc. Trans. *30*, 963–969.

Kim, H.J., Kim, N.C., Wang, Y.D., Scarborough, E.A., Moore, J., Diaz, Z., MacLea, K.S., Freibaum, B., Li, S., Molliex, A., et al. (2013). Mutations in prion-like domains in hnRNPA2B1 and hnRNPA1 cause multisystem proteinopathy and ALS. Nature *495*, 467–473.

Klionsky, D.J., Abdelmohsen, K., Abe, A., Abedin, M.J., Abeliovich, H., Acevedo Arozena, A., Adachi, H., Adams, C.M., Adams, P.D., Adeli, K., et al. (2016). Guidelines for the use and interpretation of assays for monitoring autophagy (3rd edition). Autophagy *12*, 1–222.

Kroschwald, S., Maharana, S., Mateju, D., Malinovska, L., Nüske, E., Poser, I., Richter, D., and Alberti, S. (2015). Promiscuous interactions and protein disaggregases determine the material state of stress-inducible RNP granules. eLife *4*, e06807.

Lee, G.J., and Vierling, E. (2000). A small heat shock protein cooperates with heat shock protein 70 systems to reactivate a heat-denatured protein. Plant Physiol. *122*, 189–198.

Liu-Yesucevitz, L., Bilgutay, A., Zhang, Y.J., Vanderweyde, T., Citro, A., Mehta, T., Zaarur, N., McKee, A., Bowser, R., Sherman, M., et al. (2010). Tar DNA binding protein-43 (TDP-43) associates with stress granules: analysis of cultured cells and pathological brain tissue. PLoS ONE *5*, e13250.

Lüders, J., Demand, J., and Höhfeld, J. (2000). The ubiquitin-related BAG-1 provides a link between the molecular chaperones Hsc70/Hsp70 and the proteasome. J. Biol. Chem. *275*, 4613–4617.

Mazroui, R., Di Marco, S., Kaufman, R.J., and Gallouzi, I.E. (2007). Inhibition of the ubiquitin-proteasome system induces stress granule formation. Mol. Biol. Cell *18*, 2603–2618.

Meriin, A.B., Zaarur, N., and Sherman, M.Y. (2012). Association of translation factor eEF1A with defective ribosomal products generates a signal for aggresome formation. J. Cell Sci. *125*, 2665–2674.

Minoia, M., Boncoraglio, A., Vinet, J., Morelli, F.F., Brunsting, J.F., Poletti, A., Krom, S., Reits, E., Kampinga, H.H., and Carra, S. (2014). BAG3 induces the sequestration of proteasomal clients into cytoplasmic puncta: implications for a proteasome-to-autophagy switch. Autophagy *10*, 1603–1621.

Molliex, A., Temirov, J., Lee, J., Coughlin, M., Kanagaraj, A.P., Kim, H.J., Mittag, T., and Taylor, J.P. (2015). Phase separation by low complexity domains promotes stress granule assembly and drives pathological fibrillization. Cell *163*, 123–133.

Murakami, T., Qamar, S., Lin, J.Q., Schierle, G.S., Rees, E., Miyashita, A., Costa, A.R., Dodd, R.B., Chan, F.T., Michel, C.H., et al. (2015). ALS/FTD mutation-induced phase transition of FUS liquid droplets and reversible hydrogels into irreversible hydrogels impairs RNP granule function. Neuron *88*, 678–690.

Noonan, E.J., Place, R.F., Giardina, C., and Hightower, L.E. (2007). Hsp70B′ regulation and function. Cell Stress Chaperones *12*, 219–229.

Patel, A., Lee, H.O., Jawerth, L., Maharana, S., Jahnel, M., Hein, M.Y., Stoynov, S., Mahamid, J., Saha, S., Franzmann, T.M., et al. (2015). A liquid-to-solid phase transition of the ALS protein FUS accelerated by disease mutation. Cell *162*, 1066–1077.

Poser, I., Sarov, M., Hutchins, J.R., Hériché, J.K., Toyoda, Y., Pozniakovsky, A., Weigl, D., Nitzsche, A., Hegemann, B., Bird, A.W., et al. (2008). BAC TransgeneOmics: a high-throughput method for exploration of protein function in mammals. Nat. Methods *5*, 409–415.

Robberecht, W., and Philips, T. (2013). The changing scene of amyotrophic lateral sclerosis. Nat. Rev. Neurosci. *14*, 248–264.

Schubert, U., Antón, L.C., Gibbs, J., Norbury, C.C., Yewdell, J.W., and Bennink, J.R. (2000). Rapid degradation of a large fraction of newly synthesized proteins by proteasomes. Nature *404*, 770–774.

Seguin, S.J., Morelli, F.F., Vinet, J., Amore, D., De Biasi, S., Poletti, A., Rubinsztein, D.C., and Carra, S. (2014). Inhibition of autophagy, lysosome and VCP function impairs stress granule assembly. Cell Death Differ. *21*, 1838–1851.

Selcen, D., Muntoni, F., Burton, B.K., Pegoraro, E., Sewry, C., Bite, A.V., and Engel, A.G. (2009). Mutation in BAG3 causes severe dominant childhood muscular dystrophy. Ann. Neurol. *65*, 83–89.

Sudnitsyna, M.V., Mymrikov, E.V., Seit-Nebi, A.S., and Gusev, N.B. (2012). The role of intrinsically disordered regions in the structure and functioning of small heat shock proteins. Curr. Protein Pept. Sci. *13*, 76–85.

Verma, R., Oania, R.S., Kolawa, N.J., and Deshaies, R.J. (2013). Cdc48/p97 promotes degradation of aberrant nascent polypeptides bound to the ribosome. eLife *2*, e00308.

Wegrzyn, R.D., and Deuerling, E. (2005). Molecular guardians for newborn proteins: ribosome-associated chaperones and their role in protein folding. Cell. Mol. Life Sci. *62*, 2727–2738.

Yewdell, J. (2002). To DRiP or not to DRiP: generating peptide ligands for MHC class I molecules from biosynthesized proteins. Mol. Immunol. *39*, 139–146.